Macromolecules

pubs.acs.org/Macromolecules Article

Carvacrol- and Cardanol-Containing 1,3-Dioxolan-4-ones as Comonomers for the Synthesis of Functional Polylactide-Based Materials

Stefano Gazzotti, Marco Aldo Ortenzi,* Hermes Farina, Mariapina Disimino, and Alessandra Silvani

Cite This: https://dx.doi.org/10.1021/acs.macromol.0c01537 Read Online

ACCESS | Metrics & More | Article Recommendations | Supporting Information

ABSTRACT: 1,3-Dioxolan-4-one (DOX) chemistry was exploited for the synthesis of poly(lactic acid) (PLA)-based copolymers. A new DOX monomer, bearing the naturally occurring carvacrol (CarvDOX) as a pendant, was synthesized and used as a model for the optimization of DOX-L-lactide, solvent-free, copolymerization reactions. A screening of conditions was carried out to find out the best catalytic system for both comonomers at the same time, as well as to maximize the growth of the molecular weight. The optimized copolymerization conditions were then applied to a second DOX derivative (CardDOX), bearing the naturally occurring 3-pentacylphenol (cardanol), as an appendage. Various copolymers between L-lactide and different amounts of CarvDOX or CardDOX were prepared and characterized through NMR and wide-angle X-ray scattering (WAXS), also assessing their thermal properties via differential scanning calorimetry (DSC) and thermogravimetric analysis (TGA). To exploit the potential use of such copolymers as functional additives in poly(lactic acid) (PLA), they were blended via solvent mixing with commercial PLA and the melt viscosity properties of the resulting blends were investigated through frequency sweep experiments.

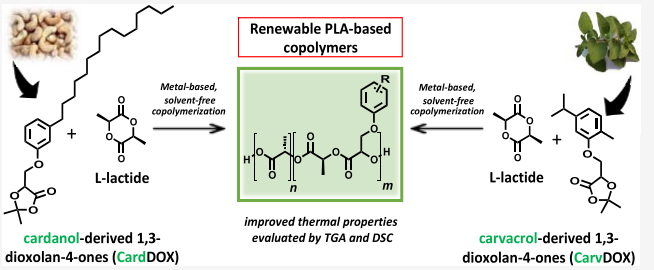

INTRODUCTION

The growing interest around poly(lactic acid) (PLA) relies on a combination of different factors. Indeed, given an increasing worldwide plastic-related pollution problem, researchers put their efforts seeking valid alternatives to replace oil-derived polymers.[1] Within this field, PLA has emerged as an intriguing candidate, thanks to the striking combination of environmentally friendly nature and desirable features, such as good processability and optical properties, that make it suitable for several industrial applications.[2] Lactic acid can be extracted 100% from renewable sources,[3] and PLA can degrade to unharmful products, therefore offering applications in biomedical and food packaging fields.[4,5] However, its intrinsic scarce versatility has always limited its industrial appeal and competitiveness against oil-derived counterparts. Among all possible strategic approaches aimed at overcoming this drawback, the chemical modification of the PLA backbone has been less investigated with respect to the preparation of nanocomposites[6,7] or blends.[8,9] In principle, the introduction of selected substituents along the polymeric chain would end up in the possible tuning of the material's final properties, expanding its scope. However, the chemical nature of PLA and, in general, of poly(α-hydroxy acids) (PAHAs), has always been a strong hurdle for targeted chemical modification.[10,11] In this regard, along with the functionalization reactions performed on the polymer, which are usually limited and relatively inefficient,[12−14] the synthesis of modified monomers has been investigated as a possible strategy.[15−17]

Within this context, the modification of lactic acid could be relatively easy and versatile. Nevertheless, the polycondensation of free lactic acid yields low molecular weight products[18] due to the difficulties in efficiently removing the water formed during polymerization. For this reason, if high molecular weight polymers are required, it is necessary to use other kinds of polymerization pathways. From an industrial standpoint, the synthesis of PLA relies on the ring-opening polymerization (ROP) of lactide, the cyclic dimer of lactic acid. However, while the ROP of lactide allows high conversion and good control over the polymerization, the synthesis of functionalized lactides is very challenging and strongly sensitive to the steric hindrance of the substituents.[19−21]

To overcome such limitations, recently Bourissou et al. developed O-carboxyanhydrides (OCAs)[22] as an alternative monomeric system, offering wide functionalization possibilities.[23−25] OCAs polymerize under mild conditions, given the strong driving force ensured by the release of CO_2 during

Received: July 3, 2020

https://dx.doi.org/10.1021/acs.macromol.0c01537
Macromolecules XXXX, XXX, XXX−XXX

polymerization.[26] However, the high reactivity of OCAs also entails an inherent instability, making these monomers difficult to handle and store. Furthermore, their synthesis relies on hazardous chemicals.

Aiming at classes of monomers that could be able to allow structural modification and good reactivity, while overcoming OCA drawbacks, 1,3-dioxolan-4-ones (DOXs) have appeared as promising candidates. DOX synthesis is straightforward from the parent α-hydroxy acid, and their high reactivity in ROP is ensured by the release of a small molecule (either aldehyde or ketone) during the ring-opening step, in a similar way as previously described for OCAs.[27] However, albeit being easily accessible molecules, the use of DOXs as monomers for the synthesis of PLA-based materials has been scarcely investigated.[28,29]

We recently studied the reactivity of a eugenol-functionalized DOX monomer, yielding a high-performance, degradable thermoset.[30] Aiming at a further expansion of DOX scope, we herein report the metal-catalyzed, solvent-free copolymerization between the commercially available L-lactide and two DOX monomers, aimed at achieving the efficient incorporation of phenol-containing units into a high molecular weight polyester chain. Screening of various metal catalytic systems was carried out using a carvacrol-functionalized DOX as a model monomer (CarvDOX). Carvacrol was chosen because it is an antimicrobial monoterpenoid phenol, naturally occurring in various essential oils, which has been already used in blending with PLA, showing effects on the thermal and mechanical properties of the resulting material.[31−35] The optimized copolymerization protocol was then applied to a second DOX monomer (CardDOX), carrying a cardanol-derived appendage. Cardanol is a phenolic lipid obtained from anacardic acid, the main component of cashew oil. Thanks to its long aliphatic side chain, cardanol has been exploited as a plasticizer within many different polymeric matrices.[36−40] Using CarvDOX and CardDOX in different quantities, several modified PLAs have been prepared, fully characterized, and studied regarding their thermal properties, through both thermogravimetric analysis (TGA) and differential scanning calorimetry (DSC). All copolymers were blended with commercial-grade PLA, and the rheological properties of the final materials were evaluated in view of the possible application of copolymers as PLA additives.

EXPERIMENTAL SECTION

Materials and Methods. All reagents were purchased from Sigma-Aldrich and used as received. (±)-3-Chloro-1,2-propanediol, 98%; HNO_3, ≥65%; carvacrol, ≥98%; HCl, ≥37%; ethyl acetate (AcOEt), H_2SO_4, 95−97%; 3-pentadecylphenol (cardanol), 90%; tin(II) 2-ethylhexanoate, 92.5−100%; zinc perchlorate hexahydrate-($Zn(ClO_4)_2$); zinc trifluoromethanesulfonate ($Zn(OTf)_2$), 98%; tin(II) chloride, 98%; magnesium perchlorate hexahydrate, 99%; methanol (MeOH); dichloromethane (DCM); dimethyl sulfoxide-d^6 (DMSO-*d*6), minimum deuteration degree 99.8%; and chloroform-d ($CDCl_3$), minimum deuteration degree 99.8%. L-Lactide Purasorb L was purchased from Corbion and used as received. Natureworks PLA Ingeo 3251D was purchased from Resinex Italy Srl.

*Synthesis of 3-Chloro-2-hydroxypropanoic Acid (**1**).* Compound (**1**) was synthesized according to the literature procedure.[41]

*Synthesis of 2-Hydroxy-3-(5-isopropyl-2-methylphenoxy)-propanoic Acid (**2**).* Carvacrol (7.2 g, 48.2 mmol) and NaOH (3.3 g, 82.5 mmol) were added to a dispersion of **1** (2.0 g, 16.1 mmol) in 20 mL of H_2O. The reaction mixture was heated to reflux and left under stirring for 4 h. The solution was then acidified to pH 1 with concentrated HCl and extracted with AcOEt (4 × 10 mL). The organic phases were collected and extracted with a saturated aqueous $NaHCO_3$ solution (4 × 10 mL). The aqueous phases were then collected, acidified with concentrated H_2SO_4 to reach pH 1, and finally extracted with AcOEt (4 × 10 mL). The organic phases were collected and dried over Na_2SO_4, and the solvent was evaporated under reduced pressure to obtain **2** as an orange solid (1.6 g, 41% yield). ^{1}H NMR (400 MHz, DMSO-d^6) δ 7.02 (d, J = 7.6 Hz, 1H), 6.79 (d, J = 1.2 Hz, 1H), 6.71 (dd, J = 7.6, 1.2 Hz, 1H), 4.36 (dd, J = 5.0, 3.6 Hz, 1H), 4.15 (ddd, J = 3.6, 5.0, 10.0 Hz, 2H), 2.83 (ept, J = 6.8 Hz, 1H), 2.09 (s, 3H), 1.18 (d, J = 6.8, 6H). ^{13}C NMR (101 MHz, DMSO-d^6) δ 173.9, 156.9, 147.9, 130.6, 123.8, 118.6, 110.5, 70.8, 70.0, 33.8, 24.4 (2C), 15.8.

Synthesis of 5-((5-Isopropyl-2-methylphenoxy)methyl)-2,2-dimethyl-1,3-dioxolan-4-one (CarvDOX). Compound **2** (2.6 g, 10.9 mmol) was dissolved in acetone (100 mL). The solution was cooled to −10 °C and then concentrated H_2SO_4 was added dropwise (4.0 mL). The reaction mixture was left under stirring for 4 h. Saturated aqueous $NaHCO_3$ was then added until pH 8 was reached. The solid was filtered off, and the solution was extracted with AcOEt (4 × 10 mL). The organic phases were collected and dried over Na_2SO_4, and the solvent was removed under reduced pressure to obtain **3** as an orange solid (2.1 g, 70% yield). ^{1}H NMR (400 MHz, $CDCl_3$) δ 7.08 (d, J = 7.6 Hz, 1H), 6.80 (dd, J = 7.6, 1.6 Hz, 1H), 6.74 (d, J = 1.6 Hz, 1H), 4.78 (dd, J = 3.6, 2.4 Hz, 1H), 4.34 (ddd, J = 2.4, 3.6, 10.8 Hz, 2H), 2.89 (ept, J = 6.8 Hz, 1H), 2.22 (s, 3H), 1.73 (s, 3H), 1.65 (s, 3H), 1.27 (d, J = 6.8 Hz, 6H). ^{13}C NMR (101 MHz, $CDCl_3$) δ 170.6, 156.3, 148.0, 130.7, 124.5, 119.2, 111.5, 110.2, 74.4, 67.0, 34.1, 27.0, 26.7, 24.1 (2C), 15.8.

*Synthesis of 2-Hydroxy-3-(3-pentadecylphenoxy)propanoic Acid (**4**).* 3-Pentadecylphenol (3.0 g, 10.0 mmol) and NaOH (1.1 g, 27.3 mmol) were dissolved in H_2O/MeOH 1:2 (4.5 mL). A solution of **1** (1.1 g, 8.8 mmol) in MeOH (1.5 mL) was added dropwise at room temperature. The reaction mixture was heated to reflux and left under stirring overnight. The reaction mixture was then cooled to room temperature and diluted with H_2O (30 mL). Unreacted 3-pentadecylphenol was then extracted with Et_2O (4 × 10 mL). After this, the aqueous phase was acidified with concentrated H_2SO_4 to pH 1 and extracted with AcOEt (4 × 10 mL). The organic phases were collected and dried over Na_2SO_4, and the solvent was evaporated under reduced pressure to obtain **4** as an orange solid (1.5 g, 43% yield). ^{1}H NMR (400 MHz, DMSO-d^6) δ 7.16 (t, J = 8.4 Hz, 1H), 6.76−6.72 (m, 3H), 4.34−4.32 (m, 1H), 4.13−4.11 (m, 2H), 2.52−2.50 (m, 2H + OH), 1.54 (s, br, 2H), 1.25 (s, br, 24H), 0.86 (t, J = 6.5 Hz, 3H). ^{13}C NMR (101 MHz, DMSO-d^6) δ 174.4, 159.6, 145.1, 130.3, 121.9, 115.7, 112.8, 71,0, 70.4, 36.3, 32.4, 32.0, 30.2−29.8 (10C), 23.2, 15.1.

Synthesis of 2,2-Dimethyl-5-((3-pentadecylphenoxy)methyl)-1,3-dioxolan-4-one (CardDOX). Compound **4** (3.0 g, 7.6 mmol) was dissolved in acetone (100 mL). The solution was cooled to −10 °C and then concentrated H_2SO_4 was added dropwise (2.0 mL). The reaction mixture was left under stirring for 4 h. Saturated aqueous $NaHCO_3$ was then added until pH 8 was reached. The solid was filtered off, and the solution was extracted with AcOEt (4 ×10 mL). The organic phases were collected and dried over Na_2SO_4, and the solvent was removed under reduced pressure to obtain **5** as an orange solid (2.1 g, 64% yield). ^{1}H NMR (400 MHz, $CDCl_3$) δ 7.21 (t, J = 8.0 Hz, 1H), 6.83 (d, J = 8.0 Hz, 1H), 6.77 (s, 1H), 6.76 (d, J = 8.0, 1H), 4.78 (dd, J = 4.0, 2.4 Hz, 1H), 4.31 (ddd, J = 10.8, 4.0, 2.4, 2H), 2.59 (t, J = 7.6 Hz, 2H), 1.72 (s, 3H), 1.64 (s, 3H), 1.64−1.60 (m, 2H), 1.29 (s, br, 24H), 0.91 (t, J = 5.6 Hz, 3H). ^{13}C NMR (101 MHz, $CDCl_3$) δ 170.5, 158.2, 144.8, 129.2, 121.8, 115.0, 111.8, 111.7, 74.3, 66.9, 36.0, 31.9, 31.4, 29.7−29.4 (10C), 27.1, 26.7, 22.7, 14.1.

Optimized Copolymerization Procedure. The selected DOX monomer of a proper amount depending on the chosen m/m% loading was placed in a 250 mL three-necked round bottom flask and dried at 60 °C overnight, under nitrogen flow. Then, L-lactide (0.1 mol), $Zn(ClO_4)_2$ (0.25 wt % with respect to the monomers), $Zn(OTf)_2$ (0.05 wt % with respect to the monomers), and $Sn(Oct)_2$ (0.03 wt % with respect to the monomers) were added and mechanical stirring was performed (40 rpm). The reaction was carried

https://dx.doi.org/10.1021/acs.macromol.0c01537
Macromolecules XXXX, XXX, XXX−XXX

Scheme 1. Reagents and Conditions: (a) Carvacrol, NaOH, H_2O, Reflux, 4h; (b) Acetone, H_2SO_4, 4h; and (c) Cardanol, NaOH, H_2O/MeOH, Reflux, Overnight

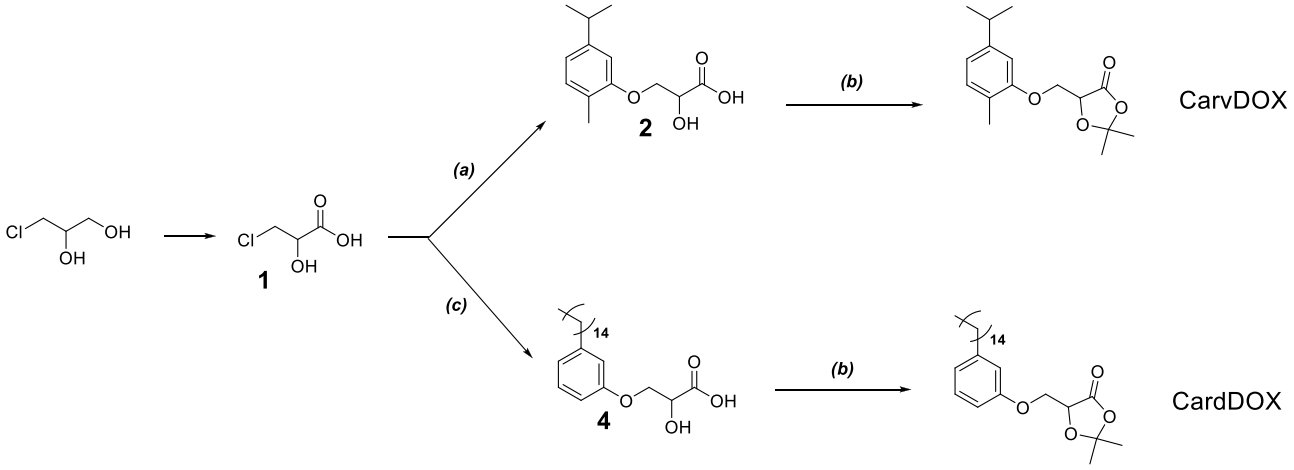

Scheme 2. Copolymerization Reaction between CarvDOX and L-Lactide

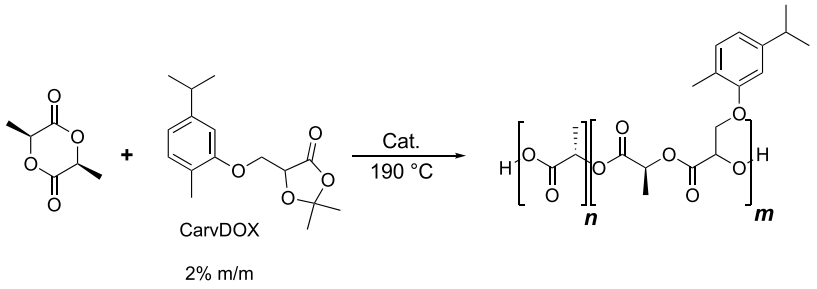

out in a closed oven at 190 °C for 4 h, and then the polymer was left for cooling overnight.

Nuclear Magnetic Resonance (NMR). ^{1}H NMR and ^{13}C NMR spectra were recorded on Bruker Ultrashield 400 or Bruker Avance 300 MHz spectrometers, at 298 K.

Size Exclusion Chromatography (SEC). The molecular weight of synthesized polymers was evaluated using a SEC system having a Waters 1515 Isocratic high-performance liquid chromatography (HPLC) pump and a four Waters Styragel column set (HR3-HR4-HR5-HR2) with a UV detector Waters 2487 Dual λ Absorbance Detector set at 230 nm, using a flow rate of 1 mL/min and 60 μL as the injection volume. The samples were prepared by dissolving 50 mg of polymer in 1 mL of anhydrous CH_2Cl_2 and filtering the solution on 0.45 μm filters. Given the relatively high loading, a check was performed using a lower concentration of polymer (5 mg/mL) to verify that no column overloading was observed. Higher loadings were preferred as the UV signal of PLA is relatively weak. Molecular weight data are expressed in polystyrene (PS) equivalents. The calibration was built using 16 monodispersed PS standards, having a peak molecular weight ranging from 1 600 000 Da to 106 g/mol (i.e., ethylbenzene). For all analyses, 1,2-dichlorobenzene was used as an internal reference.

Thermogravimetric Analysis (TGA). TGA was performed using a TGA 4000 Perkin Elmer instrument. Tests were conducted under a nitrogen atmosphere on samples weighing from 5 to 10 mg each, with a program that provides a single heating cycle from 30 to 650 °C at 20 °C/min.

Differential Scanning Calorimetry (DSC). DSC analyses were conducted using a Mettler Toledo DSC1 on samples weighing from 5 to 10 mg each. Melting and crystallization temperatures were measured using the following temperature cycles: (1) heating from 25 to 200 °C at 10 °C/min; (2) cooling from 200 to 25 °C at 10 °C/min; (3) heating from 25 to 70 °C at 10 °C/min; and (4) heating from 70 to 200 °C at 5 °C/min. The first two cycles were run to erase the thermal history of the samples. Glass transition temperature (T_g), cold crystallization temperature (T_{cc}), and melting temperature (T_m) were determined during the second heating scan.

Wide-Angle X-ray Scattering (WAXS). Wide-Angle X-ray Scattering (WAXS) experiments were performed using a Rigaku DMAX-II diffractometer. Diffraction patterns were obtained in the range $5° < 2\theta < 50°$ with Cu Kα radiation (λ = 1.5405 Å) under the following conditions: 40 kV, 40 mA, step width 0.02°, time per step 2 s, divergence slit 0.25°, Soller slit 0.04 rad, and antiscatter slit 0.5°.

Preparation of Blends and Films. Blends between synthesized samples and PLA Ingeo 3251D were prepared through solvent mixing using chloroform as a solvent. The samples were dissolved in a 10% w/w ratio with Ingeo 3251D. One gram in the total of the material was dissolved into 15 mL of $CHCl_3$ at 30 °C. Once dissolution was complete, solutions were cast on a glass surface and the solvent was evaporated at room temperature and pressure overnight. Film samples were then kept in a vacuum at 25 °C for 3 days. Complete evaporation of the solvent was checked through TGA analysis.

Rheological Analyses. Rheological analyses, conducted using frequency sweep experiments, were performed using a Physica MCR 300 rotational rheometer with a parallel plate geometry (diameter = 25 mm, the distance between plates = 1 mm). Linear viscoelastic regimes of neat Ingeo 3251D and blends were studied; strain was set equal to 5% and curves of complex viscosity, storage, and loss modulus as a function of frequency were recorded, taking 30 points ranging from 100 to 0.1 Hz with a logarithmic progression, at 180 °C.

Zero shear viscosity (η_0) values were calculated using a cross equation passing from experimental data obtained as complex viscosity (η^*) versus angular frequency to data as shear viscosity versus shear rate, thanks to the Cox–Merz rule.

https://dx.doi.org/10.1021/acs.macromol.0c01537
Macromolecules XXXX, XXX, XXX−XXX

Table 1. Screening of Conditions for L-Lactide−CarvDOX Copolymerization

entry	reaction time (h)	catalyst	catalyst loading (wt %)	% reacted CarvDOX[a]	% unreacted L-lactide[b]	$\overline{M_w}$ (g/mol)[c]	Đ
1	2	$Sn(Oct)_2$	0.30	0	0	52 600	1.7
2	2	$SnCl_2$	0.30	10	0	43 000	1.6
3	2	$Zn(ClO_4)_2$	0.30	100	54	5700	1.6
4	2	$Mg(OCl_4)_2$	0.3	100	80	oligomers	
5	2	$SnCl_2$	0.15	47	5	21 400	1.5
		$Zn(ClO_4)_2$	0.15				
6	2	$SnCl_2$	0.10	36	8	19 700	1.6
		$Zn(ClO_4)_2$	0.20				
7	2	$SnCl_2$	0.05	44	12	15 100	1.8
		$Zn(ClO_4)_2$	0.25				
8	6	$Zn(ClO_4)_2$	0.3	100	30	15 200	2.4
9	6	$Zn(ClO_4)_2$	0.2	100	13	13 900	1.5
		$Zn(OTf)_2$	0.1				
10	6	$Zn(ClO_4)_2$	0.25	100	11	14 500	1.7
		$Zn(OTf)_2$	0.05				
11	6	$Zn(ClO_4)_2$	0.15	100	17	14 300	1.4
		$Zn(OTf)_2$	0.15				
12[d]	6	$Zn(ClO_4)_2$	0.20	100	2	5000	1.9
		$Zn(OTf)_2$	0.10				
13[d]	6	$Zn(ClO_4)_2$	0.25	100	2	5300	1.9
		$Zn(OTf)_2$	0.05				
14[d]	6	$Zn(ClO_4)_2$	0.15	100	2	2600	1.5
		$Zn(OTf)_2$	0.15				
15[d]	6	$Zn(ClO_4)_2$	0.25	100	10	16 200	2.3
		$Zn(OTf)_2$	0.05				
		$Sn(Oct)_2$	0.01				
16[d]	6	$Zn(ClO_4)_2$	0.25	100	5	17 800	2.5
		$Zn(OTf)_2$	0.05				
		$Sn(Oct)_2$	0.03				
17[d]	2	$Zn(ClO_4)_2$	0.25	100	24	9700	1.5
		$Zn(OTf)_2$	0.05				
		$Sn(Oct)_2$	0.03				
18[d]	4	$Zn(ClO_4)_2$	0.25	100	3	18 400	2.4
		$Zn(OTf)_2$	0.05				
		$Sn(Oct)_2$	0.03				

[a]Determined through ^{1}H NMR spectroscopy as a ratio between the signal at 5.55 ppm and the sum of signals at 4.78 and 5.55 ppm in the final product. [b]Determined through ^{1}H NMR spectroscopy as the ratio between the signal at 5.08 ppm and the sum of signals at 5.08 and 5.19 ppm in the final product. [c]Determined through SEC analysis against a PS calibration. [d]Reactions performed with dried $Zn(ClO_4)_2$.

RESULTS AND DISCUSSION

Synthesis of DOX Monomers. The synthesis of monomers relies on the direct functionalization of β-chlorolactic acid **1**, using two different naturally occurring phenols, as shown in Scheme 1.

The preparation of compound **2** was straightforward, according to conditions similar to those already reported in a previous paper.[30] The synthesis of compound **4** proved to be more challenging, given the strong apolar character of cardanol. In this case, it was necessary to add methanol as a cosolvent to ensure the complete solubility of sodium phenolate in the aqueous environment and to carry out alkylation, albeit in moderate yield. CarvDOX and CardDOX monomers were obtained straightforwardly, from α-hydroxy acids **2** and **4**, respectively.

L-Lactide−CarvDOX Copolymerization Reaction: Screening of Conditions. Using CarvDOX as a model monomer, all reactions were carried out with a 2% m/m DOX to L-lactide ratio, at 190 °C, under a nitrogen atmosphere (Scheme 2). The samples were analyzed through ^{1}H NMR and SEC to determine the conversion (with respect to both L-lactide and DOX) and the molecular weight of the products. Given the low quantity of DOX used, hydrodynamic volumes of the copolymers obtained were considered to be identical to the ones of PLA homopolymers: molecular weight data obtained via SEC were therefore compared with no further adjustments.

To find out the best conditions for the reaction of both monomers, different catalytic systems, catalyst to monomer ratios, and reaction times were evaluated (Table 1). At first, different metal-based catalysts were selected with the aim to determine the most active one toward DOX polymerization. With $Sn(Oct)_2$, which is the catalyst of choice for the ROP of L-lactide, no reaction of the DOX monomer was detected, while L-lactide reacted completely (entry **1**). With the more Lewis acidic $SnCl_2$[42] (entry **2**), a modest conversion of the DOX monomer was detectable, showing a possible correlation between the Lewis acidic character of the catalyst and the interaction with 1,3-dioxolan-4-one. Given the well-known activity of zinc-based catalysts toward L-lactide, cheap $Zn(ClO_4)_2$ was evaluated[43] (entry **3**). This catalyst proved its effectiveness toward the DOX monomer, ensuring its complete

https://dx.doi.org/10.1021/acs.macromol.0c01537
Macromolecules XXXX, XXX, XXX−XXX

conversion, but did not catalyze the ring-opening of L-lactide, thus conducting to a low molecular weight polymer. $Mg(ClO_4)_2$[44] gave similar results, affording complete DOX conversion, but only oligomers, because of the very low reactivity of L-lactide (entry **4**). Given the higher tendency of DOX and L-lactide to react in the presence of zinc- and tin-based catalysts, respectively, a mixture of $Zn(ClO_4)_2$ and $SnCl_2$ was tested, in different ratios (entries **5**, **6**, and **7**). In all cases, the combination of the two catalysts allowed obtaining high conversions of L-lactide and up to 47% conversion of the DOX monomer. Considering the effectiveness of zinc-based catalysts toward **3**, $Zn(ClO_4)_2$ was tested again, increasing the reaction time, to encourage the L-lactide reaction (entry **8**). The reaction gave higher molecular weight products with respect to entry **3**, even if unreacted L-lactide was still present in considerable amounts. Once the need for longer reaction times was realized, the following tests were carried out over a period of 6 h. To further increase L-lactide reactivity, $Zn(ClO_4)_2$ was tested in combination with the more Lewis acidic $Zn(OTf)_2$,[44] in different ratios (entries **9**, **10**, and **11**). All three reactions showed a complete conversion of **3**, with L-lactide conversion improving as well. Aiming at evaluating the effects of $Zn(ClO_4)_2$ hydration water, this catalyst was subjected to a dehydration protocol,[45,46] before being used for copolymerization. As reported in entries **12**, **13**, and **14**, in addition to the complete conversion of **3**, the use of a dried catalyst led to an almost complete conversion of L-lactide. Surprisingly, however, molecular weights of the products dropped significantly, probably due to transesterification/backbiting reactions, occurring at long reaction times, in the presence of the more active dried catalysts. To counterbalance this effect, small quantities of $Sn(Oct)_2$ were added to the catalytic system, finally resulting in relatively high molecular weight products and good conversions for both monomers (entries **15** and **16**). With the best combination of catalysts in hand (entry **16**), a conclusive optimization was pursued, comparing different reaction times. While an incomplete reaction was detected in 2 h (entry **17**), the optimal sweet spot, in terms of highly satisfactory conversion of both monomers and molecular weight of the product, was obtained in 4 h (entry **18**).

L-Lactide−CarvDOX Copolymerization Reaction: Evaluation of Monomer Reactivity and Molecular Weight Growth. The L-lactide−CarvDOX copolymerization reaction was carried out for 4 h at 190 °C under the optimized conditions, as reported in Table 1, entry **18**, with samples taken at given times. The samples were frozen in liquid nitrogen as soon as they were taken, to stop the reaction. All samples were analyzed through ^{1}H NMR and SEC, to evaluate the conversion of the two monomers, as well as the molecular weight growth. Stacked ^{1}H NMR spectra for all samples are reported in Figure 1 with magnifications of the areas of interest. The reaction was considered to start upon reaching 190 °C, and the first sample was taken at that moment. Its ^{1}H NMR spectrum shows a signal at 4.61 ppm due to the partial deprotection of the DOX monomer. This signal decreases sharply in the following spectra (10, 20, 30 min), suggesting an early consumption of unprotected DOX, which was likely acting as a polymerization initiator. The formation of a polymerization product is highlighted by the appearance and increasing intensity of a broad signal between 5.49 and 5.65 ppm, which is attributable to the -CH- group in the DOX-derived repeating unit. After 45 min, the DOX monomer methine group signal was no more detectable, while unreacted

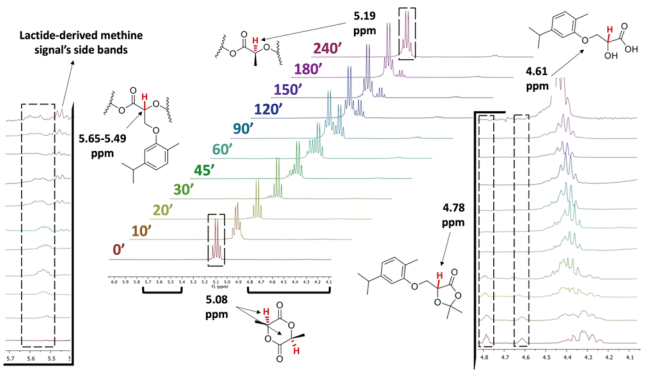

Figure 1. Stacked ^{1}H NMR spectra recorded at 300 MHz for all samples taken during the L-lactide−CarvDOX copolymerization with magnifications of the 5.71−5.40 and 4.82−4.05 ppm regions.

L-lactide (quartet at 5.08, CH) was still predominant. The signal relative to L-lactide-derived repeating units (quartet at 5.19, CH) started to be visible at 20 min reaction time and increased in intensity throughout the reaction, up to 4 h.

Several studies on lactide ROP kinetics describe the evolution of the polymer molecular weight with time as affected by many different factors, such as temperature, kind of the catalyst, and the monomer to initiator ratio. In addition, backbiting side-reactions can take place. These intramolecular transesterification reactions are fairly common in the ROP of lactide and become more significant at high temperatures and long reaction times, resulting in a decrease of the molecular weight due to the formation of cyclic oligomers.[47−50] As shown in Figure 2, in the L-lactide−CarvDOX copolymerization described herein, two different trends can be highlighted, namely, a fast increase of the molecular weight in the early reaction stages, followed by a slowdown after 60 min reaction time. The fast increase of the molecular weight at the beginning of the reaction can be explained by the high initiation and propagation rates at a high monomer concentration. On the other hand, the increase of the molecular weight generates an increase of the viscosity of the melt, which hinders the heat and mass transfer, slowing down the macromolecular chains' growth.

The continuous, albeit slower, increase of the molecular weight up to 4 h, demonstrate a limited occurrence of backbiting side-reactions.

L-Lactide−CarvDOX Copolymerization Reaction: Optimization of CarvDOX Loading. Under the above reported optimized conditions, different reactions were carried out, varying the CarvDOX loading (2, 4, 10, and 20 mol %, with respect to L-lactide). Crude polymerization products were analyzed to determine the possible presence of unreacted monomers. Stacked ^{1}H NMR spectra in the ppm range of interest are reported in Figure 3 (for the whole spectra, see the Supporting Information).

The signals relative to the CH group in DOX-derived polymeric units are visible between 5.49 and 5.65 ppm in all spectra. DOX appeared to be fully reacted up to 4% m/m CarvDOX, while some unreacted monomer was still present in the final material, for reactions conducted at 10 and 20% m/m loading (signal at 4.78 ppm). This incomplete insertion was explained by a possible deactivation of the catalyst at high DOX concentrations. Table 2 reports a ^{1}H NMR-based evaluation of the mol % of CarvDOX-derived repeating units in the final polymer and the molecular weight data relative to

https://dx.doi.org/10.1021/acs.macromol.0c01537
Macromolecules XXXX, XXX, XXX−XXX

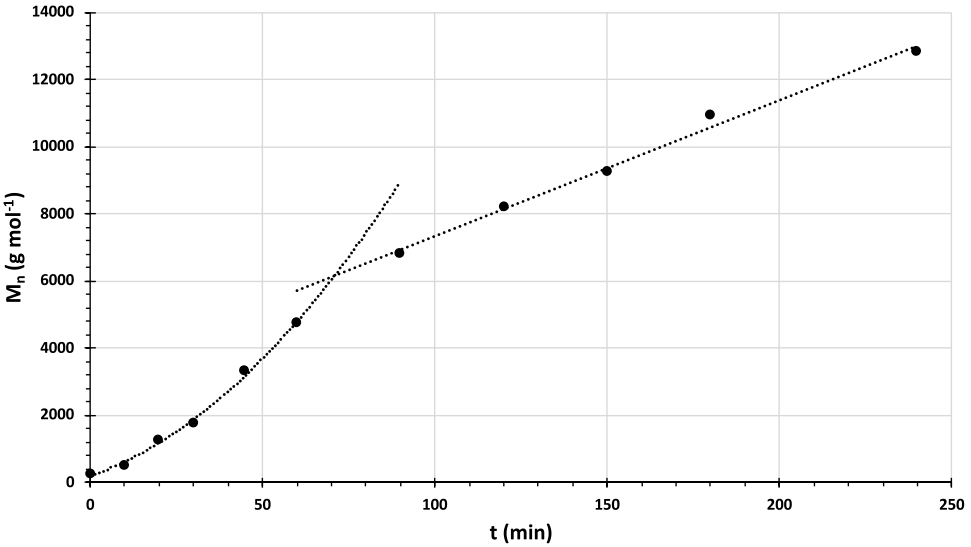

Figure 2. Increase of the molecular weight over time for the L-lactide−CarvDOX copolymerization.

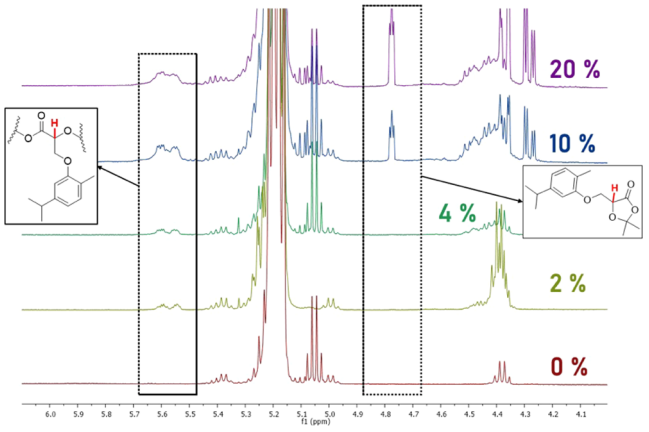

Figure 3. Stacked ^{1}H NMR spectra recorded at 400 MHz of crude products at different CarvDOX loadings.

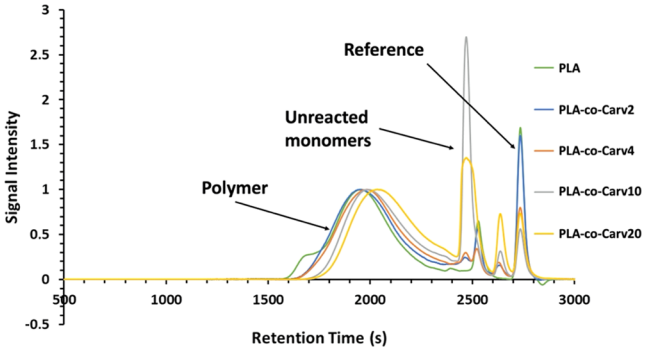

Figure 4. SEC traces relative to standard PLA and L-lactide−CarvDOX copolymers.

all copolymers compared to a standard PLA, synthesized in the same conditions.

Superimposed SEC traces for all samples are reported in Figure 4, showing a decrease of the final copolymer molecular weight with an increase in the CarvDOX loading. As highlighted above (Figure 1), CarvDOX deprotects at early reaction stages, releasing free α-hydroxy acids that can likely act as initiators. As the initial loading of the CarvDOX monomer increases, the concentration of α-hydroxy acids increases as well, ending up in a final lower molecular weight. In addition, the possible, progressive deactivation of the catalyst with the increasing DOX concentration may likely have a detrimental effect on the molecular weight growth.

L-Lactide−CardDOX Copolymerization Reaction. The protocol optimized for the L-lactide−CarvDOX copolymerization was then applied to the reaction of the CardDOX monomer. Copolymerizations with 2, 4, 10, and 20 mol % of CardDOX with respect to L-lactide were performed. Stacked ^{1}H NMR of the crude products in the ppm range of interest are compared in Figure 5 (for whole spectra, see the Supporting Information).

Furthermore, for the reaction of CarvDOX, the presence of the L-lactide−CardDOX copolymerization product can be deduced from the broad signal at 5.49−5.65 ppm, which is

Table 2. ^{1}H-NMR-Based Evaluation of the Mol % of CarvDOX-Derived Repeating Units in the Final Copolymers. Molecular Weight Data of Copolymers Compared to a Standard PLA

sample	monomer loading (mol %)	reacted monomer (mol %)[a]	$\overline{M_n}$ (g/mol)[b]	$\overline{M_w}$ (g/mol)[b]	M_p (g/mol)[b]	$Đ$
PLA			10 000	19 000	15 000	1.9
PLA-*co*-Carv2	2	2.0	10 000	20 000	15 000	2.0
PLA-*co*-Carv4	4	4.0	7000	17 000	12 000	2.2
PLA-*co*-Carv10	10	6.0	6000	13 000	12 000	2.2
PLA-*co*-Carv20	20	11.2	6000	10 000	9000	1.7

[a]Determined through ^{1}H NMR spectroscopy as a ratio between signals at 5.55 and 5.19 ppm in the final product. [b]Determined through SEC against a PS calibration.

https://dx.doi.org/10.1021/acs.macromol.0c01537
Macromolecules XXXX, XXX, XXX−XXX

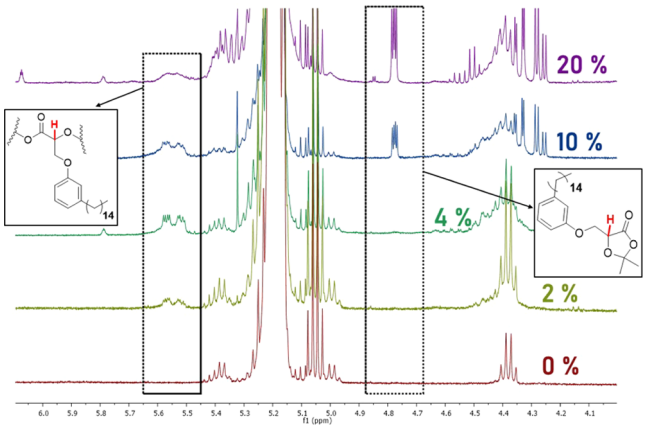

Figure 5. Stacked ^{1}H NMR spectra recorded at 400 MHz of crude products at different CardDOX loadings.

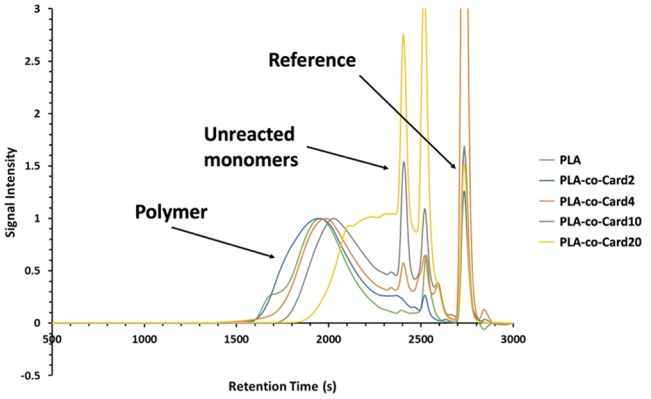

Figure 6. SEC traces relative to standard PLA and L-lactide−CardDOX copolymers.

referred to the CH of CardDOX in the polymerized units. Also, in this case, when higher CardDOX loadings were tested, some unreacted monomer was detectable at the end of the reaction, as highlighted by the signal centered at 4.77 ppm. Table 3 reports the ^{1}H NMR-based evaluation of the mol % of CarvDOX-derived repeating units in the final polymer and the molecular weight data relative to all copolymers compared to a standard PLA.

The reactivity of the CardDOX monomer appeared to be comparable to that of CarvDOX, with residual, unreacted monomer still present, when used at higher loading.

Superimposed SEC traces for all samples are reported in Figure 6. As already observed for L-lactide−CarvDOX copolymerization, also in this case, the molecular weight of the products decreases with the increasing DOX monomer loading. Such a decrease can be due to not only the presence of DOX-deprotected species acting as initiators, as already proposed for the L-lactide−CarvDOX copolymerization, but also, in this case, due to the peculiar hydrophobic nature of the cardanol-derived moiety, which likely causes progressive phase separation between the growing chain and the free monomer, indeed acting as a hurdle for the chain growth.

Investigation of the Microstructures of Copolymers. Once the optimized reaction conditions were proven effective for the copolymerization of DOX monomers and L-lactide, a preliminary investigation of the microstructure of the polymer was carried out. As shown in Figure 1, both monomers react during the early reaction stages, suggesting the formation of a random copolymer. From a stereochemical point of view, reactions were carried out between enantiomerically pure L-lactide and racemic DOX monomers. For this reason, the random reaction of L-lactide with either (R)- or (S)-DOX, would end up in the generation of a stereochemical disorder.

To investigate this aspect further, ^{1}H NMR spectra were recorded decoupling from the methyl signal at 1.56 ppm. PLA-*co*-Carv10 and PLA-*co*-Card10 were chosen as model samples and compared to standard PLA. Magnifications of the three spectra in the decoupled methine region are reported in Figure 7.

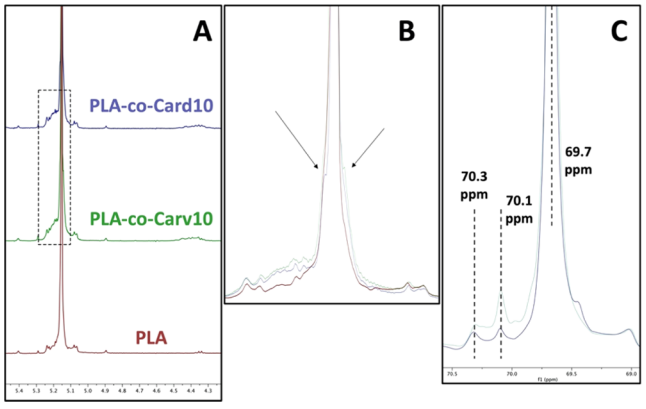

Figure 7. Stacked (A) and superimposed (B) homonuclear decoupled ^{1}H NMR spectra recorded at 300 MHz in the methine region of PLA-*co*-Card10, PLA-*co*-Carv10, and PLA samples, normalized with respect to the main peak at 5.15 ppm. Superimposed ^{13}C NMR spectra in the methine region of PLA-*co*-Card10 and PLA-*co*-Carv10 samples (C).

Figure 7A reports the stacked spectra of the three samples, showing a main singlet at 5.15 ppm, related to methine protons of the stereoregular L-lactide-derived units. Both copolymers

Table 3. 1H-NMR-Based Evaluation of the mol % of CardDOX-Derived Repeating Units in the Final Copolymers. Molecular Weight Data of Copolymers Compared to a Standard PLA

sample	monomer loading (mol %)	reacted monomer (mol %)[a]	$\overline{M_n}$ (g/mol)[b]	$\overline{M_w}$ (g/mol)[b]	M_p (g/mol)[b]	$Đ$
PLA			10 000	19 000	15 000	1.9
PLA-*co*-Card2	2	2.0	11 000	26 000	16 000	2.5
PLA-*co*-Card4	4	4.0	10 000	19 000	13 000	1.9
PLA-*co*-Card10	10	8.4	7000	11 000	9000	1.7
PLA-*co*-Card20	20	9.5	oligomers	oligomers		

[a]Determined through ^{1}H NMR spectroscopy as a ratio between signals at 5.55 and 5.19 ppm in the final product. [b]Determined through SEC against a PS calibration.

https://dx.doi.org/10.1021/acs.macromol.0c01537
Macromolecules XXXX, XXX, XXX−XXX

show broadening at 5.15−5.25 ppm, not detectable in the PLA spectrum. This broadening is likely related to the presence of different tetrads,[51−54] generated by the random succession of L-lactide and (*R*)- or (*S*)-DOX-derived units, similar to that observed in the spectra of (*rac*)-lactide polymerization products.

In Figure 7B, the same spectra were superimposed. The broadening at 5.15−5.25 ppm appears to have a comparable intensity for both PLA-*co*-Card10 and PLA-*co*-Carv10 samples. Moreover, the main peak at 5.15 ppm of the two copolymers is not as sharp as the one detected for the PLA sample, showing shoulders that could be still attributed to the stereochemical disorder.

Superimposed ^{13}C NMR spectra in the methine region are reported in Figure 7C. The main peak at 69.7 ppm is related to the methine groups of the stereoregular polymer regions derived from enantiopure L-lactide. The two minority peaks at 70.3 and 70.1 ppm further confirm the generation of random sequences of L-lactide and (R)- or (S)-DOX-derived units during the copolymerization reaction.

Thermal Characterization of L-Lactide−CarvDOX and L-Lactide−CardDOX Copolymers. Before thermal analysis, all samples were dissolved in a minimum amount of DCM, precipitated in cold MeOH, and analyzed through ^1H NMR to assess the complete removal of unreacted species. The two samples derived from 20 mol % DOX loading (i.e., PLA-*co*-Carv20 and PLA-*co*-Card20) did not precipitate, probably because of the low molecular weight and, therefore, were not characterized through TGA and DSC analyses.

TGA Analyses. TGA analyses were performed to determine the thermal stability of copolymers, with respect to a standard PLA synthesized in the same reaction conditions. For a direct comparison among all samples, temperatures corresponding to the 5, 50, and 95% weight loss were chosen and labeled as $T_{5\%}$, $T_{50\%}$, and $T_{95\%}$, respectively. TGA thermograms for all samples are reported in the Supporting Information, while the relative data are summarized in Table 4.

Table 4. Thermal Degradation Data Relative to Synthesized PLA-*co*-Carv and PLA-*co*-Card Copolymers

sample	$T_{5\%}$ (°C)	$T_{50\%}$ (°C)	$T_{95\%}$ (°C)
PLA	272.1	329.6	356.7
PLA-*co*-Carv2	278.1	337.7	371.1
PLA-*co*-Carv4	276.8	319.2	343.0
PLA-*co*-Carv10	271.1	317.2	344.3
PLA-*co*-Card2	270.7	313.1	333.1
PLA-*co*-Card4	267.3	311.3	333.5
PLA-*co*-Card10	263.2	300.0	320.6

PLA-*co*-Carv2 and PLA-*co*-Carv4 show a slight increase in thermal stability, with $T_{5\%}$ higher up to 6 °C over standard PLA. Remarkably, PLA-*co*-Carv2 appears more stable along the entire thermal degradation pathway, with $T_{95\%}$ being 14 °C higher than the one of standard PLA. PLA-*co*-Carv4 and PLA-*co*-Carv10 degrade faster once the degradation starts. It should be noted that PLA-*co*-Carv10 shows comparable thermal stability with respect to the PLA sample, albeit having a significantly lower molecular weight. It is worth mentioning that the weight loss of more classical PLA-carvacrol blends starts at temperatures lower than 200 °C.[31,34] This behavior is partly attributed to the evaporation of the free carvacrol dispersed within the matrix and also to an actual degradation of the chains, promoted by the slightly acidic phenol moieties.

PLA-*co*-Card copolymers show a different behavior: their thermal stability is slightly lower than the one of PLA and gets lower as the quantity of cardanol increases. $T_{5\%}$ of all samples is anyway far higher than T_m of PLA, confirming an overall good thermal stability of PLA-*co*-Card copolymers. As already observed for PLA-carvacrol blends, also previously reported PLA-cardanol blends have significantly lower thermal stability with respect to standard PLA.[39,40] Therefore, even if the overall thermal stabilities of the copolymers are lower than those of standard PLA (with the exception of PLA-*co*-Carv2), these findings appear remarkable if compared with those reported from the previous literature related to blending strategies. In addition, all samples start to degrade at temperatures higher than the melting temperature of PLA, opening possibilities for melt mixing processing. In particular, as both carvacrol[31−35] and cardanol[36−40] are known as biobased PLA additives for the tuning of thermal properties, the usage of such copolymers would guarantee optimal compatibility and dispersion within the matrix, overcoming the common hurdles to the use of phenols as additives for PLA-based materials.

DSC Analyses. DSC thermograms for all samples are reported in the Supporting Information, while the relative data are summarized in Table 5. Glass transition temperature T_g, cold crystallization temperature T_{CC}, and melting temperature T_m refer to the transitions occurring during the second heating scan.

Table 5. DSC Data Relative to the Second Heating Scans for Synthesized PLA-*co*-Carv and PLA-*co*-Card Copolymers

sample	T_g (°C)	T_{CC} (°C)	T_m (°C)	
PLA	57	100	170	
PLA-*co*-Carv2	56	121	149	156
PLA-*co*-Carv4	57	114	140	149
PLA-*co*-Carv10	55			
PLA-*co*-Card2	52		150	
PLA-*co*-Card4	51		152	
PLA-*co*-Card10	44			

PLA-*co*-Carv2 and PLA-*co*-Carv4 are semicrystalline polymers with T_g similar to that of standard PLA. The cold crystallization peak for both samples was detected at temperatures higher than the ones of PLA, and the melting peak was split, indicating the presence of two distinct crystalline phases. Both the higher T_{CC} with respect to PLA and the splitting of the melting peak can be ascribed to the presence of more disordered crystal structures due to the hindering effect of carvacrol-derived side groups. It has been reported[55] that PLA generates stable crystals, labeled as α-crystals, when crystallizing from the melt. A disordered crystalline form (known as α') can arise when structural elements preventing an efficient crystallization are present. Being less ordered, α' crystals melt at lower temperatures with respect to standard α ones. In PLA-*co*-Carv, the presence of bulky carvacrol-derived side moieties likely interacts with PLA crystallization, resulting in the formation of a double crystalline phase. The increased chain disorder was confirmed by the thermogram of PLA-*co*-Carv10. While T_g remains almost constant, the material appeared to be completely amorphous,

https://dx.doi.org/10.1021/acs.macromol.0c01537
Macromolecules XXXX, XXX, XXX−XXX

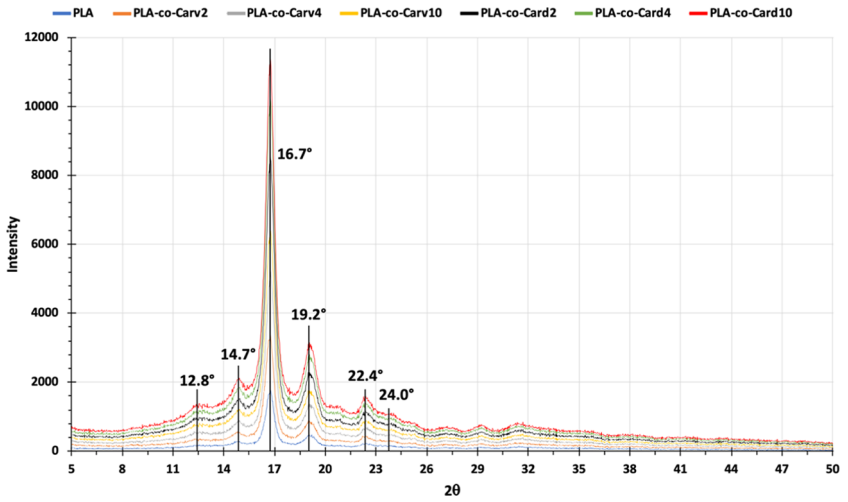

Figure 8. WAXS diffractograms for all synthesized samples.

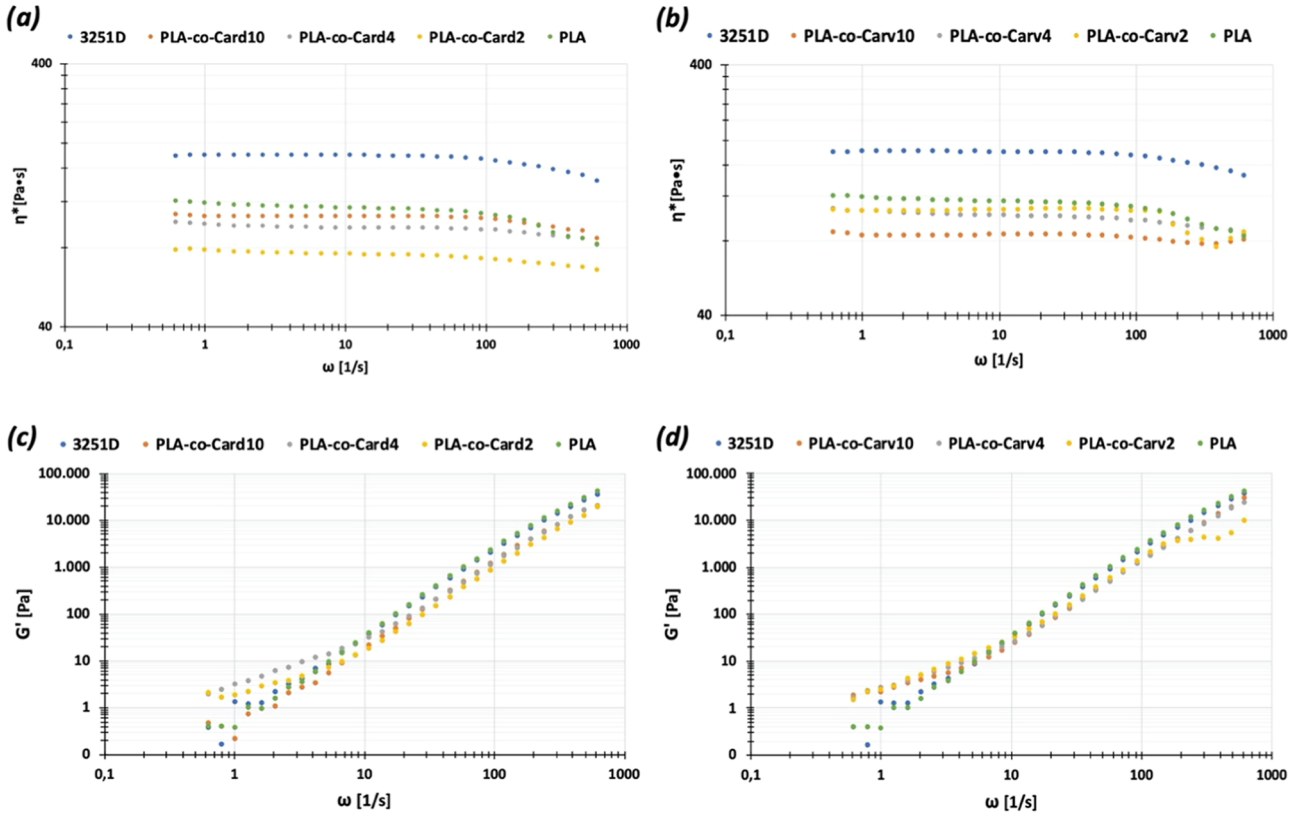

Figure 9. (a) Complex viscosity curves of cardanol-containing blends compared to Ingeo 3251D; (b) complex viscosity curves of carvacrol-containing blends compared to Ingeo 3251D; (c) storage modulus curves of cardanol-containing blends compared to Ingeo 3251D; (d) storage modulus curves of carvacrol-containing blends compared to Ingeo 3251D.

as a result of the increased quantity of bulky substituents hindering an efficient crystallization.

Cardanol-derived copolymers show a different behavior, with all three samples (i.e., PLA-*co*-Card2, PLA-*co*-Card4, and PLA-*co*-Card10) displaying a decrease of T_g, up to 13 °C less than standard PLA. Having similar molecular weights, this highlights the effects exerted in the presence of cardanol-derived side chains on the glass transition temperature of the product. With regard to the crystallization behavior, both PLA-*co*-Card2 and PLA-*co*-Card4 show very broad, hardly detectable cold crystallization peak, followed by a broad melting peak with low intensity. As already observed for PLA-*co*-Carv samples, the presence of bulky substituents hinders proper crystallization, which is even more difficult in PLA-*co*-Card, given the presence of the long cardanol-derived side chain. In fact, PLA-*co*-Card10 appeared to be fully amorphous.

Wide-Angle X-ray Scattering (WAXS). WAXS analyses were performed to further investigate the effects of the carvacrol and cardanol-derived side chains on the crystallinity of the obtained materials. Figure 8 reports the stacked diffractograms for all samples, with the main peaks highlighted.

https://dx.doi.org/10.1021/acs.macromol.0c01537
Macromolecules XXXX, XXX, XXX−XXX

WAXS diffractograms for each sample are reported in the Supporting Information file. All samples are characterized by a well-defined diffraction pattern, which is associated with an ordered α-crystalline phase.[56] In particular, the two most intense peaks, namely, at 2θ = 16.7 and 19.2°, can be ascribed to the (110)/(200) and (203) lattice planes, respectively. Also, less intense peaks at 2θ = 12.8, 14.7, and 22.4° can be attributed to the α-phase. It was reported that the α- and the less ordered α'-phases are characterized by similar diffraction patterns, with the most significant difference being a weak scattering peak at $2\theta \approx 24.0°$ for the α'-phase.[57] All samples show a small peak at $2\theta \approx 24.0°$, which becomes more intense with the increase of the DOX-derived unit concentration, parallel to the second melting peak in DSC data, and in accordance with a progressive rise of the α'-crystalline phase. Clearly, the disorder imparted by the bulky aromatic side groups translates to less crystalline materials. In particular, WAXS diffractograms show a broadening of the peaks as the DOX-derived unit concentration increases, pointing out a more significant contribution of the amorphous phase.

Rheological Analyses. Given the relatively low molecular weight and good thermal properties, CarvDOX and CardDOX-derived copolymers could be used as functional additives in PLA-based materials, ensuring high compatibility and preventing the possible leakage over time of phenols which, as such, are scarcely compatible with PLA. To assess this potential, PLA-*co*-Carv and PLA-*co*-Card were blended with a commercial injection molding grade PLA, Ingeo 3251D, and the effects exerted by the aromatic side groups of copolymers on the melt rheology of the final blends were investigated, focusing on complex viscosity η^*, storage modulus G', and loss modulus G''. Figure 9 reports the rheological curves obtained through frequency sweep experiments for all samples. Graphs relative to complex viscosity (panels a and b) and storage modulus (panels c and d) are presented, while loss modulus graphs are reported in the Supporting Information file.

All blends show a typical pseudoplastic behavior with a Newtonian plateau at low shear rates. As expected, melt viscosities are lower than that of the commercial PLA used as the matrix, but they fall in the same range. Table 6 reports the

Table 6. η_0 Values for all Tested Samples

sample	η^0 [Pa s]
3251D	178
PLA	120
PLA-*co*-Card10	106
PLA-*co*-Card4	100
PLA-*co*-Card2	79
PLA-*co*-Carv10	85
PLA-*co*-Carv4	106
PLA-*co*-Carv2	106

η_0 values obtained for all blends. Interestingly, among cardanol-derived blends (panel **a**), the PLA-*co*-Card10 blend shows a higher viscosity than PLA-*co*-Card4 and PLA-*co*-Card2 blends, despite being based on the lowest molecular weight copolymer. This might be related to the higher concentration of long aliphatic side chains of cardanol. On the other hand, carvacrol-derived blends (panel **b**) display decreasing viscosity with decreasing molecular weight of copolymers, as expected.

Storage modulus curves show a typical pseudoplastic behavior for all samples. G' appears to decrease in the 100 to 10 s^{-1} range, following a linear trend. At frequencies lower than 10 s^{-1} Ingeo 3251D and most of the blends have storage modulus values that become too low to be accurately measured by the instrument.

CONCLUSIONS

The applicability of 1,3-dioxolan-4-ones (DOXs) as functional comonomers for the synthesis of PLA-based materials was demonstrated. Two naturally occurring phenols (i.e., carvacrol and cardanol) were chosen for DOX functionalization, given their wide application as additives in many different polymeric matrices when tuning of the thermal and rheological properties is required. Carvacrol-derived DOX (CarvDOX) was selected as the model comonomer, and screening of copolymerization conditions with L-lactide was carried out. A solvent-free protocol, using a triad of metal catalysts, was developed and then applied to the synthesis of a series of copolymers, varying the starting CarvDOX loading and also using the alternative cardanol-derived DOX (CardDOX). The limits of the protocol were pointed out at high DOX concentrations, probably due to a deactivation of the catalytic system. NMR studies were carried out aiming at the determination of the microstructures of copolymers, and the formation of random copolymers was demonstrated. Then, the thermal properties of the synthesized copolymers were investigated, demonstrating the positive effect of 2% carvacrol-derived units on thermal stability, as well as the lowering of T_g due to the cardanol-derived side chains. By means of wide-angle X-ray scattering analyses, the effects of the carvacrol and cardanol-derived side chains on the crystallinity of the obtained materials were deepened. Finally, the potential application of the synthesized copolymers as additives for PLA was investigated through the preparation of blends and the study of their rheological properties. All blends show a typical pseudoplastic behavior, with PLA-*co*-Card10 blend displaying an optimal balance between melt viscosity and the content of cardanol-derived units, which witness the potential of this copolymer as a PLA additive for tuning of the final material properties.

ASSOCIATED CONTENT

Supporting Information

The Supporting Information is available free of charge at https://pubs.acs.org/doi/10.1021/acs.macromol.0c01537.

^{1}H and ^{13}C NMR spectra of monomers and precursors; ^{1}H NMR spectra relative to CarvDOX and CardDOX loading evaluation; homonuclear decoupled ^{1}H NMR spectra and ^{13}C NMR spectra for microstructure determination; TGA curves, DSC thermograms; WAXS diffractograms; loss modulus curves (PDF)

AUTHOR INFORMATION

Corresponding Author

Marco Aldo Ortenzi − *Dipartimento di Chimica and CRC Materiali Polimerici "LaMPo", Dipartimento di Chimica, Università degli Studi di Milano, 20133 Milano, Italy;* orcid.org/0000-0001-6206-9589; Email: marco.ortenzi@unimi.it

Authors

Stefano Gazzotti − *Dipartimento di Chimica and CRC Materiali Polimerici "LaMPo", Dipartimento di Chimica,*

https://dx.doi.org/10.1021/acs.macromol.0c01537
Macromolecules XXXX, XXX, XXX−XXX

Università degli Studi di Milano, 20133 Milano, Italy; orcid.org/0000-0001-5287-711X

Hermes Farina − *Dipartimento di Chimica and CRC Materiali Polimerici "LaMPo", Dipartimento di Chimica, Università degli Studi di Milano, 20133 Milano, Italy*

Mariapina Disimino − *Dipartimento di Chimica and CRC Materiali Polimerici "LaMPo", Dipartimento di Chimica, Università degli Studi di Milano, 20133 Milano, Italy*

Alessandra Silvani − *Dipartimento di Chimica and CRC Materiali Polimerici "LaMPo", Dipartimento di Chimica, Università degli Studi di Milano, 20133 Milano, Italy;* orcid.org/0000-0002-0397-2636

Complete contact information is available at: https://pubs.acs.org/10.1021/acs.macromol.0c01537

Notes

The authors declare no competing financial interest.

■ ACKNOWLEDGMENTS

The authors wish to thank Professor Giordano Lesma for his countless suggestions and advice, as well as for his unparalleled knowledge, which he has always been eager to share.

■ REFERENCES

(1) Bandelli, D.; Alex, J.; Weber, C.; Schubert, U. S. Polyester Stereocomplexes Beyond PLA: Could Synthetic Opportunities Revolutionize Established Material Blending? *Macromol. Rapid Commun.* **2020**, *41*, No. e1900560.

(2) Tsuji, H.; Ikada, Y. Blends of Aliphatic Polyesters. I. Physical Properties and Morphologies of Solution-Cast Blends frorn Poly(Dilactide) and Poly(c-caprolactone). *J. Appl. Polym. Sci.* **1996**, *6*, 2367−2375.

(3) Gao, C.; Ma, C.; Xu, P. Biotechnological routes based on lactic acid production from biomass. *Biotechnol. Adv.* **2011**, *29*, 930−939.

(4) Auras, R.; Harte, B.; Selke, S. An Overview of Polylactides as Packaging Materials. *Macromol. Biosci.* **2004**, *4*, 835−864.

(5) Albertsson, A. C.; Hakkarainen, M. Designed to degrade. *Science* **2017**, *358*, 872−873.

(6) Gazzotti, S.; Farina, H.; Lesma, G.; Rampazzo, R.; Piergiovanni, L.; Ortenzi, M. A.; Silvani, A. Polylactide/cellulose nanocrystals: The in situ polymerization approach to improved nanocomposites. *Eur. Polym. J.* **2017**, *94*, 173−184.

(7) Gazzotti, S.; Rampazzo, R.; Hakkarainen, M.; Bussini, D.; Ortenzi, M. A.; Farina, H.; Lesma, G.; Silvani, A. Cellulose nanofibrils as reinforcing agents for PLA-based nanocomposites: An in situ approach. *Compos. Sci. Technol.* **2019**, *171*, 94−102.

(8) Liu, H.; Chen, N.; Shan, P.; Song, P.; Liu, X.; Chen, J. Toward Fully Bio-based and Supertough PLA Blends via in Situ Formation of Cross-Linked Biopolyamide Continuity Network. *Macromolecules* **2019**, *52*, 8415−8429.

(9) Przybysz-Romatowska, M.; Haponiuk, J.; Formela, K. Poly(ε-Caprolactone)/Poly(Lactic Acid) Blends Compatibilized by Peroxide Initiators: Comparison of Two Strategies. *Polymers* **2020**, *12*, 228.

(10) Rasal, R. M.; Janorkarc, A. V.; Hirt, D. E. Poly(lactic acid) modifications. *Prog. Polym. Sci.* **2010**, *35*, 338−356.

(11) Becker, G.; Wurm, F. R. Functional biodegradable polymers via ring-opening polymerization of monomers without protective groups. *Chem. Soc. Rev.* **2018**, *47*, 7739−7782.

(12) Stoleru, E.; Dumitriu, R. P.; Munteanu, B. S.; Zaharescu, T.; Tanase, E. E.; Mitelut, A.; Ailieseia, G. L.; Vasile, C. Novel procedure to enhance PLA surface properties by chitosan irreversible immobilization. *Appl. Surf. Sci.* **2016**, *367*, 407−417.

(13) Wang, S.; Cui, W.; Bei, J. Bulk and surface modifications of polylactide. *Anal Bioanal Chem* **2005**, *381*, 547−556.

(14) Standau, T.; Zhao, C.; Castellón, S. M.; Bonten, C.; Altstädt, V. Chemical Modification and Foam Processing of Polylactide (PLA). *Polymers* **2019**, *11*, 306.

(15) Wright, C.; Banerjee, A.; Yan, X.; Storms-Miller, W. K.; Pugh, C. Synthesis of Functionalized Poly(lactic acid) Using 2-Bromo-3-hydroxypropionic Acid. *Macromolecules* **2016**, *49*, 2028−2038.

(16) Abtew, E.; Ezra, A. F.; Basu, A.; Domb, A. J. Biodegradable Poly(Acetonide Gluconic Acid) for Controlled Drug Delivery. *Biomacromolecules* **2019**, *20*, 2934−2941.

(17) Ndugire, W.; Wu, B.; Yan, M. Synthesis of Carbohydrate-Grafted Glycopolymers Using a Catalyst-Free, Perfluoroarylazide-Mediated Fast Staudinger Reaction. *Molecules* **2019**, *24*, 157.

(18) Marques, D. S.; Gil, M. H.; Baptista, C. M. S. G. Improving Lactic Acid Melt Polycondensation: The Role of Co-Catalyst. *J. Appl. Polym. Sci.* **2013**, 2145−2151.

(19) Sun, H.; Chang, M. Y. Z.; Cheng, W.; Wang, Q.; Commisso, A.; Capeling, M.; Wu, Y.; Cheng, C. Biodegradable zwitterionic sulfobetaine polymer and its conjugate with paclitaxel for sustained drug delivery. *Acta Biomater.* **2017**, *64*, 290−300.

(20) Kalelkar, P.; Collard, D. M. Thiol-substituted copolylactide: synthesis, characterization and post-polymerization modification using thiol−ene chemistry. *Polym. Chem.* **2018**, *9*, 1022−1031.

(21) Fuoco, T.; Pappalardo, D.; Finne-Wistrand, A. Redox-Responsive Disulfide Cross-Linked PLA−PEG Nanoparticles. *Macromolecules* **2017**, *50*, 7052−7061.

(22) Martin Vaca, B. M.; Bourissou, D. O-Carboxyanhydrides: Useful Tools for the Preparation of Well- Defined Functionalized Polyesters. *ACS Macro Lett.* **2015**, *4*, 792−798.

(23) Gazzotti, S.; Todisco, S. A.; Picozzi, C.; Ortenzi, M. A.; Farina, H.; Lesma, G.; Silvani, A. Eugenol-grafted aliphatic polyesters: Towards inherently antimicrobial PLA-based materials exploiting OCAs chemistry. *Eur. Polym. J.* **2019**, *114*, 369−379.

(24) Cui, Y.; Jiang, J.; Pan, X.; Wu, J. Highly isoselective ring-opening polymerization of rac-O-carboxyanhydrides using a zinc alkoxide initiator. *Chem. Commun.* **2019**, *55*, 12948−12951.

(25) Li, M.; Tao, Y.; Tang, J.; Wang, Y.; Zhang, X.; Tao, Y.; Wang, X. Synergetic Organocatalysis for Eliminating Epimerization in Ring-Opening Polymerizations Enables Synthesis of Stereoregular Isotactic Polyester. *J. Am. Chem. Soc.* **2019**, *141*, 281−289.

(26) Thillaye du Boullay, O. T.; Marchal, E.; Vaca, B. M.; Cossio, F. P.; Bourissou, D. An Activated Equivalent of Lactide toward Organocatalytic Ring-Opening Polymerization. *J. Am. Chem. Soc.* **2006**, *128*, 16442−16443.

(27) Xu, Y.; Perry, M. R.; Cairns, S. A.; Shaver, M. P. Understanding the ring-opening polymerisation of dioxolanones. *Polym. Chem.* **2019**, *10*, 3048−3054.

(28) Cairns, S. A.; Schultheiss, A.; Shaver, M. P. A broad scope of aliphatic polyesters prepared by elimination of small molecules from sustainable 1,3-dioxolan-4-ones. *Polym. Chem.* **2017**, *8*, 2990−2996.

(29) Martin, R. T.; Camargo, L. P.; Miller, S. A. Marine-degradable polylactic acid. *Green Chem.* **2014**, *16*, 1768−1773.

(30) Gazzotti, S.; Hakkarainen, M.; Adolfsson, K. H.; Ortenzi, M. A.; Farina, H.; Lesma, G.; Silvani, A. One-Pot Synthesis of Sustainable High-Performance Thermoset by Exploiting Eugenol Functionalized 1,3-Dioxolan-4-one. *ACS Sustainable Chem. Eng.* **2018**, *6*, 15201−15211.

(31) Celebi, H.; Gunes, E. Combined effect of a plasticizer and carvacrol and thymol on the mechanical, thermal, morphological properties of poly(lactic acid). *J. Appl. Polym. Sci.* **2018**, *135*, No. 45895.

(32) Scaffaro, R.; Lopresti, F. Processing, structure, property relationships and release kinetics of electrospun PLA/Carvacrol membranes. *Eur. Polym. J.* **2018**, *100*, 165−171.

(33) Burgos, N.; Armentano, I.; Fortunati, E.; Dominici, F.; Luzi, F.; Fiori, S.; Cristofaro, F.; Visai, L.; Jiménez, B.; Kenny, J. M. Functional Properties of Plasticized Bio-Based Poly(Lactic Acid) _Poly-(Hydroxybutyrate) (PLA_PHB) Films for Active Food Packaging. *Food Bioprocess. Technol.* **2017**, *10*, 770−780.

(34) Requena, R.; Vargas, M.; Chiralt, A. Obtaining antimicrobial bilayer starch and polyester-blend films with carvacrol. *Food Hydrocolloids* **2018**, *83*, 118−133.
(35) Scaffaro, R.; Maio, A.; Lopresti, F. Effect of graphene and fabrication technique on the release kinetics of carvacrol from polylactic acid. *Compos. Sci. Technol.* **2019**, *169*, 60−69.
(36) Massaro, M.; Colletti, C. G.; Noto, R.; Riela, S.; Poma, P.; Guernelli, S.; Parisi, F.; Milioto, S.; Lazzara, G. Pharmaceutical properties of supramolecular assembly of co-loaded cardanol/triazole-halloysite systems. *Int. J. Pharm.* **2015**, *478*, 476−485.
(37) Greco, A.; Ferrari, F.; Maffezzoli, A. Processing of Super Tough Plasticized PLA by Rotational Molding. *Adv. Polym. Technol.* **2019**, *2019*, No. 3835829.
(38) Rigoussen, A.; Raquez, J. M.; Dubois, P.; Verge, P. A dual approach to compatibilize PLA/ABS immiscible blends with epoxidized cardanol derivatives. *Eur. Polym. J.* **2019**, *114*, 118−126.
(39) Kang, H.; Li, Y.; Gong, M.; Guo, Y.; Guo, Z.; Fang, Q.; Li, X. An environmentally sustainable plasticizer toughened polylactide. *RSC Adv.* **2018**, *8*, 11643−11651.
(40) Mele, G.; Bloise, E.; Cosentino, F.; Lomonaco, D.; Avelino, F.; Marcianò, T.; Massaro, C.; Mazzetto, S.; Tammaro, L.; Scalone, A. G.; Schioppa, M.; Terzi, R. Influence of Cardanol Oil on the Properties of Poly(lactic acid) Films Produced by Melt Extrusion. *ACS Omega* **2019**, *4*, 718−726.
(41) Zhang, X.; Dai, Y. A Functionalized Cyclic Lactide Monomer for Synthesis of Water-Soluble Poly(Lactic Acid) and Amphiphilic Diblock Poly(Lactic Acid). *Macromol. Rapid Commun.* **2016**, *38*, No. 1600593.
(42) Somekawa, S.; Masutani, K.; Hsu, Y.; Mahara, A.; Kimura, Y.; Yamaoka, T. Size-Controlled Nanomicelles of Poly(lactic acid)−Poly(ethylene glycol) Copolymers with a Multiblock Configuration. *Polymers* **2015**, *7*, 1177−1191.
(43) Bartoli, G.; Boeglin, J.; Bosco, M.; Locatelli, M.; Massaccesi, M.; Melchiorre, P.; Sambri, L. Highly Efficient Solvent-Free Condensation of Carboxylic Acids with Alcohols Catalysed by Zinc Perchlorate Hexahydrate, $Zn(ClO_4)_2 \cdot 6\ H_2O$. *Adv. Synth. Catal.* **2005**, *347*, 33−38.
(44) Shivani; Pujala, S. B.; Chakraborti, A. K. Zinc(II) Perchlorate Hexahydrate Catalyzed Opening of Epoxide Ring by Amines: Applications to Synthesis of (RS)/(R)-Propranolols and (RS)/(R)/(S)-Naftopidils. *J. Org. Chem.* **2007**, *72*, 3713−3722.
(45) Nikitina, Z. K.; Chuprakov, Y. V.; Rosolovskii, V. Y. Anhydrous zinc perchlorate and perchloratozincates. *Zhh. Neorg. Khim.* **1986**, *31*, 691−7.
(46) Pascal, J. L.; Favier, F. Inorganic perchlorato complexes. *Coord. Chem. Rev.* **1998**, *178*, 865−902.
(47) Metkar, S.; Sathe, V.; Rahman, I.; Idage, B.; Idage, S. Ring opening polymerization of lactide: kinetics and modeling. *Chem. Eng. Commun.* **2019**, *206*, 1159−1167.
(48) Yu, I.; Ramírez, A. A.; Mehrkhodavandi, P. Mechanism of Living Lactide Polymerization by Dinuclear Indium Catalysts and Its Impact on Isoselectivity. *J. Am. Chem. Soc.* **2012**, *134*, 12758−12773.
(49) Mazarro, R.; Gracia, I.; Rodrìguez, J. F.; Storti, G.; Morbidelli, M. Kinetics of the ring-opening polymerization of D,L-lactide using zinc (II) octoate as catalyst. *Polym. Int.* **2012**, *61*, 265−273.
(50) Yu, Y.; Storti, G.; Morbidelli, M. Ring-Opening Polymerization of L,L-Lactide: Kinetic and Modeling Study. *Macromolecules* **2009**, *42*, 8187−8197.
(51) Gao, B.; Duan, Q.; Li, Y.; Li, D.; Zhang, L.; Cui, Y.; Hu, N.; Pang, X. Stereoselective ring-opening polymerization of rac-lactides catalyzed by titanium complexes containing N,N-bidentate phenanthrene derivatives. *RSC Adv.* **2015**, *5*, 13437−13442.
(52) Schindler, A.; Harper, D. Poly(Lactic Acid). I. Stereosequence Distribution In The Polymerization Of Racemic Dilactide. *J. Polym. Sci., Polym. Lett. Ed.* **1976**, *14*, 729−734.
(53) Beament, J.; Mahon, M. F.; Buchard, A.; Jones, M. D. Aluminum Complexes of Monopyrrolidine Ligands for the Controlled Ring-Opening Polymerization of Lactide. *Organometallics* **2018**, *37*, 1719−1724.
(54) Suganuma, K.; Matsuda, H.; Cheng, H. N.; Iwai, M.; Nonokawa, R.; Asakura, T. NMR analysis and tacticity determination of poly(lactic acid) in C_5D_5N. *Polym. Test.* **2014**, *38*, 35−39.
(55) Cocca, M.; Di Lorenzo, M. L.; Malinconico, M.; Frezza, V. Influence of crystal polymorphism on mechanical and barrier properties of poly(L-lactic acid). *Eur. Polym. J.* **2011**, *47*, 1073−1080.
(56) Wasanasuk, K.; Tashiro, K.; Hanesaka, M.; Ohhara, T.; Kurihara, K.; Kuroki, R.; Tamada, T.; Ozeki, T.; Kanamoto, T. Crystal Structure Analysis of Poly(L-lactic Acid) α Form On the basis of the 2-Dimensional Wide-Angle Synchrotron X-ray and Neutron Diffraction Measurements. *Macromolecules* **2011**, *44*, 6441−6452.
(57) Di Lorenzo, M. L.; Androsch, R. Influence of α'-/α-crystal polymorphism on properties of poly(L-lactic acid). *Polym. Int.* **2019**, *68*, 320−334.

https://dx.doi.org/10.1021/acs.macromol.0c01537
Macromolecules XXXX, XXX, XXX−XXX